

Multidimensional Interpolants

Dohoon Lee*
IPAI
Seoul National University
ryan0919@snu.ac.kr

Kyogu Lee
IPAI
Seoul National University
kglee@snu.ac.kr

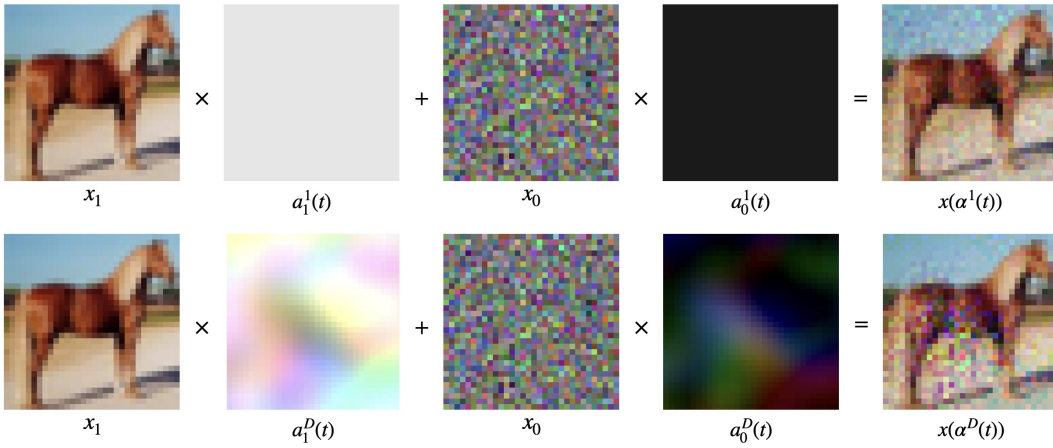


Figure 1: Comparison of interpolation methods in differential equation-based generative modeling: single-dimensional interpolant (top) vs. multidimensional interpolant (bottom). The conventional approach utilizes single-dimensional coefficients, characterized by a single scalar value for training—a method commonly employed in existing flow and diffusion models. Conversely, our methodology employs multidimensional coefficients for both training and inference.

Abstract

In the domain of differential equation-based generative modeling, conventional approaches often rely on single-dimensional scalar values as interpolation coefficients during both training and inference phases. In this work, we introduce, for the first time, a multidimensional interpolant that extends these coefficients into multiple dimensions, leveraging the stochastic interpolant framework. Additionally, we propose a novel path optimization problem tailored to adaptively determine multidimensional inference trajectories, with a predetermined differential equation solver and a fixed number of function evaluations. Our solution involves simulation dynamics coupled with adversarial training to optimize the inference path. Notably, employing a multidimensional interpolant during training improves the model’s inference performance, even in the absence of path optimization. When the adaptive, multidimensional path derived from our optimization process is employed, it yields further performance gains, even with fixed solver configurations. The introduction of multidimensional interpolants not only enhances the efficacy of models but also opens up a new domain for exploration in training and inference methodologies, emphasizing the potential of multidimensional paths as an untapped frontier.

1 Introduction

Differential equation-based generative modeling has become a cornerstone in the realm of generative modeling, demonstrating unprecedented efficacy that has facilitated its widespread adoption. Research in this domain has primarily divided into two streams: models based on ordinary differential equations (ODEs), which emphasize flow processes [1, 2], and those based on stochastic differential equations (SDEs) that focus on diffusion mechanisms [3]. Among these advancements, the study of stochastic interpolant (SI) [4, 5] has introduced a novel framework that effectively bridges the gap between flow and diffusion models. This framework not only integrates flow and diffusion mechanisms but also distinctly separates model training from path design, conventionally intertwined processes. Our work concentrates on two critical aspects of SI:

1. SI models are trained to output the mean values of target data distributions by receiving interpolated values between distributions and their corresponding interpolation coefficients.
2. SI postpones the design of inference paths until after model training, thereby enabling subsequent path optimization.

A unique feature of SI enables the utilization of multidimensional interpolation coefficients, which contrast with the conventional use of single-dimensional scalar values. For instance, in image generation, it requires learning a mapping function from a Gaussian distribution $x_0 \sim \mathcal{N}(0, I)$ to an image distribution $x_1 \sim \rho_1$, where both x_0 and x_1 are D -dimensional vectors within the real space \mathbb{R}^D . The interpolation used in SI model training is described by:

$$x(\alpha^d) = a_0^d x_0 + a_1^d x_1, \tag{1}$$

where $\alpha^d = (a_0^d, a_1^d) \in \mathbb{R}^{2 \times d}$ represents the interpolation coefficients. Conventional research in flow and diffusion has primarily focused on scenarios where $d = 1$. However, our study introduces the use of multidimensional interpolants, specifically by setting $d = D$, allowing the model to explore interpolation across various dimensions within data distributions. This method significantly broadens the spectrum of interpolation coefficients that the model needs to learn, thereby deepening its understanding of data distributions. Notably, employing multidimensional interpolation coefficients in training improves the model’s Fréchet Inception Distance (FID) scores, even when using simple linear paths without path optimization during inference.

The second key feature of SI is the enablement of inference path optimization. We explored the question: "Given a differential equation solver operating with a fixed number of function evaluations (NFE), which multidimensional path would yield optimal performance when the starting point x_0 is specified?" To address this, we utilized a GAN-based adversarial training approach, as pioneered by Goodfellow et al. [6]. This setup includes a pre-trained network g_{θ_0} trained with multidimensional interpolation coefficients, a neural network-parameterized path p_{θ_1} , and a solver engaging in simulation dynamics, with a discriminator evaluating the outcomes to facilitate path optimization. Our experiments demonstrate that paths optimized through this methodology significantly enhance the FID scores compared to those of linear paths during inference.

In summary, our **main contributions** are as follows:

1. We are the first to apply multidimensional interpolants in training differential equation-based generative models, enhancing model performance.
2. Our use of multidimensional interpolants reveals the potential of multidimensional inference paths, capitalizing on the enhanced flexibility afforded by these coefficients in training g_{θ_0} .
3. We introduce a novel path optimization problem and its solution, combining simulation dynamics with adversarial training to enable adaptive pathfinding for efficient inference.

By pioneering the use of multidimensional interpolation coefficients, our work expands the landscape of differential equation-based generative modeling and suggests new avenues for future research and application.

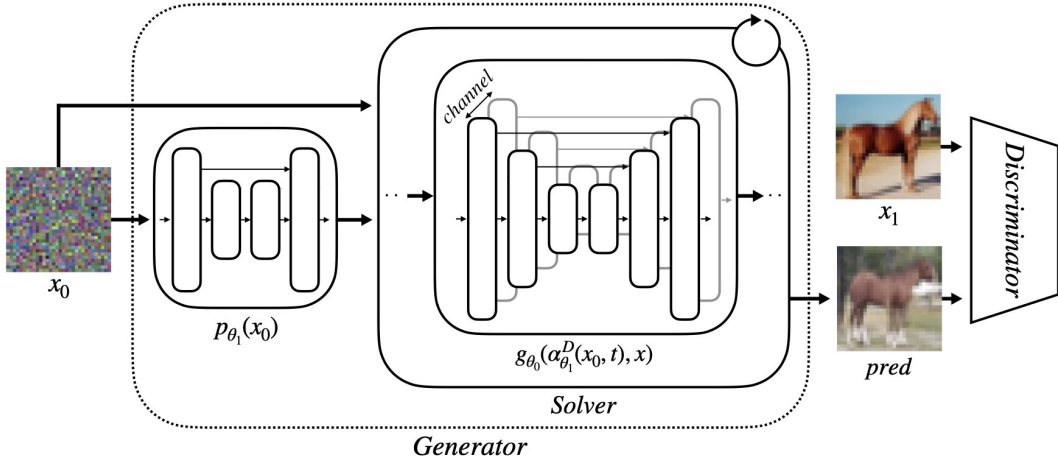


Figure 2: Path optimization process. The path, denoted as $\alpha_{\theta_1}^D(x_0, t)$, is parameterized via a Fourier expansion, with Fourier coefficients generated by $p_{\theta_1}(x_0)$. During this process, g_{θ_0} remains frozen. The solver then iteratively computes predictions ($pred$) using g_{θ_0} from the initial point x_0 . Subsequently, both x_1 and $pred$ are input into the discriminator to compute the adversarial loss.

2 Related works

Differential equation-based generative modeling Prior to the introduction of diffusion models, continuous normalizing flows (CNFs) [7], were widely adopted in differential equation-based generative modeling. In the training of CNFs, the methodology starts with an initial state x_0 and aims to reach a final state x_1 through simulation dynamics. A distinctive feature of this approach is its direct modeling of the target probability distribution ρ_1 , using likelihood as the direct loss metric. However, this approach is computationally inefficient and often performs poorly. Subsequently, score-based generative modeling [3], which pre-defines a stochastic differential equation (SDE) path and trains the score value of that path using a simulation-free dynamic, demonstrated remarkable performance. Following the score-based diffusion models, ordinary differential equation (ODE)-based methods emerged. Referred to as flow-based modeling [1, 2], these methods employ CNFs in a simulation-free dynamic similar to diffusion. Thus, differential equation-based modeling was largely divided into ODE-based flow and SDE-based diffusion, and studies like SF^2M [8] and stochastic interpolant (SI) [4] that aim to integrate these methodologies appeared. These frameworks address the transport problem by enabling transitions from any distribution to any other, overcoming the limitations of previous studies confined to Gaussian starting distributions. Later, SI was generalized in a multimarginal setting [5], presenting a comprehensive framework for differential equation-based generative modeling.

Path optimizations in differential equation-based generative modeling Path optimizations in differential equation-based generative modeling are largely divided into two main directions. Firstly, there exists a method of path optimization that defines the pair (x_0, x_1) used in training beforehand, thereby maintaining consistent pairing to straighten the path and improve the model’s inference performance with fewer NFE. For example, Liu et al. [2] identifies pairs through simulation dynamics and retrains the model with these to straighten the path. Also, Tong et al. [9] calculates optimal transport pairs on a minibatch basis using the Wasserstein distance for training. Similarly, Goldstein et al. [10] creates coupling by adding noise to x_1 . Secondly, there are methods that define and train models based on their own definitions of the optimal path. Shaul et al. [11] defines optimal paths based on kinetic energy and uses them for model training. Albergo et al. [5] defines optimal paths with the least path length in the Wasserstein-2 metric and conducts path optimization after model training. Although path optimization has been discussed from several perspectives, there has not been a proper discussion on which path to choose in terms of the quality of the generated output when the starting point x_0 is given while both the solver and the NFE are fixed. In this context, we distinguish ourselves from existing studies by addressing such path optimization issues.

3 Preliminaries: stochastic interpolants

Considering a dataset comprised of n samples, $\{x_1^i\}_{i=1}^n \subset \mathbb{R}^D$, where each $x_1 \sim \rho_1(x_1)$, and Gaussian noise $x_0 \sim \mathcal{N}(0, I)$ with $\rho_0(x_0) = \mathcal{N}(0, I)$, we introduce a time-dependent stochastic process that interpolates between ρ_0 and ρ_1 . This follows Albergo et al. [4].

Definition 1. *stochastic interpolant* $x(\alpha^d(t))$ is defined as:

$$x(\alpha^d(t)) = a_0^d(t)x_0 + a_1^d(t)x_1, \quad (2)$$

where $\alpha^d(t) = (a_0^d(t), a_1^d(t)) \in \mathbb{R}^{2 \times d}$ are differentiable functions within the interval $t \in [0, 1]$, adhering to the conditions $a_0^d(0) = a_1^d(1) = 1$ and $a_0^d(1) = a_1^d(0) = 0$, ensuring $a_0^d(t) + a_1^d(t) = 1$ and $a_0^d(t), a_1^d(t) \geq 0$.

This allows the probability distribution of $x(\alpha^d(t))$ to embody a time-dependent density $\rho(t, x)$, interpolating between $\rho_0(0, x)$ and $\rho_1(1, x)$, facilitating generative models through g described below.

Definition 2. *The conditional expectation, represented by g_0 and g_1 are expressed as:*

$$g_0(\alpha^d(t), x) = \mathbb{E}(x_0 | x(\alpha^d(t)) = x), \quad g_1(\alpha^d(t), x) = \mathbb{E}(x_1 | x(\alpha^d(t)) = x), \quad (3)$$

where \mathbb{E} is the expectation over $\rho(x_0, x_1)$ given $x(\alpha^d(t)) = x$.

For modeling g with neural network g_θ , it is essential to consider the following theorem.

Theorem 1. *The density $\rho(t, x)$ satisfies the transport equation:*

$$\partial_t \rho(t, x) + \nabla \cdot (b(t, x)\rho(t, x)) = 0, \quad (4)$$

with the velocity field b :

$$b(t, x) = \dot{a}_0^d(t)g_0(\alpha^d(t), x) + \dot{a}_1^d(t)g_1(\alpha^d(t), x). \quad (5)$$

Also, the score function when $a_0^d(t) \neq 0$ is given by:

$$\nabla \log \rho(t, x) = -(a_0^d(t))^{-1}g_0(\alpha^d(t), x). \quad (6)$$

The g_0 and g_1 uniquely minimize the following objectives:

$$L_k(\hat{g}_k) = \int_0^1 \mathbb{E}[|\hat{g}_k(\alpha^d(t), x(\alpha^d(t)))|^2 - 2x_k \cdot \hat{g}_k(\alpha^d(t), x(\alpha^d(t)))]dt, \quad k = 0, 1, \quad (7)$$

where the expectation \mathbb{E} is taken over $(x_0, x_1) \sim \rho(x_0, x_1)$.

The velocity field b corresponds to the following probability flow equation:

$$\dot{x}_t = b(t, x_t). \quad (8)$$

All methods that can be described by the aforementioned stochastic interpolant framework, which encompasses both flow and diffusion models, have thus far been defined for the case where $d = 1$.

4 Multidimensional interpolants

Using a stochastic interpolant framework, we employ a multidimensional interpolant to extend the dimensions of the coefficients $\alpha^d(t)$ to match the dimensionality of x_0 and x_1 , setting $d = D$. Additionally, we execute a path optimization process to find an adaptive multidimensional path. These processes unfold in two primary stages. Initially, in the first stage, the model g_{θ_0} is trained to approximate g_0 and g_1 as described in Equation 3. Subsequently, in the second stage, path optimization using simulation dynamics and adversarial training proceeds with g_{θ_0} frozen, the parameterized path p_{θ_1} conditioned on the initial condition x_0 , and both the solver and the number of function evaluations (NFE) fixed. This setup allows for focused optimization of the adaptive path while keeping all other factors constant.

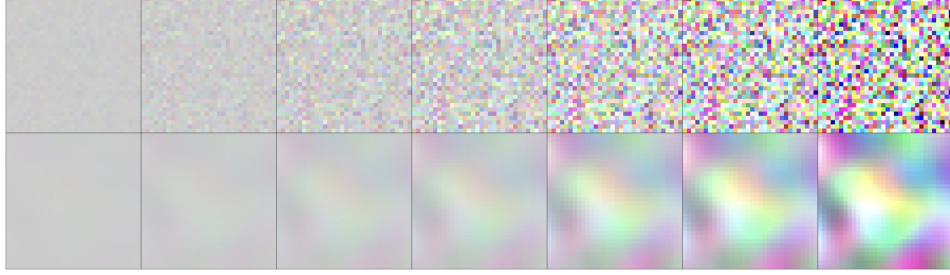


Figure 3: Gaussian-noised interpolant (GNI) and low-pass filtered interpolant (LPFI) displayed according to scale parameters $s = [0.01, 0.03, 0.06, 0.1, 0.2, 0.3, 0.5]$ from left to right.

4.1 Design choices of multidimensional interpolants

The performance of g_{θ_0} can be significantly influenced by the choice of multidimensional interpolants used for training. An overly expansive coverage by the multidimensional interpolant leads to an increased learning space for the model, thereby imposing a burden on it. Conversely, excessively narrow coverage yields outcomes indistinguishable from those obtained through the use of single-dimensional scalar value coefficients. Therefore, choosing coefficients within an optimal range is crucial. To achieve this, we propose two design strategies:

Example 1. *The Gaussian-noised interpolant is described by:*

$$a_1^D(t) = \text{clip}(t + s \cdot z, 0, 1), \quad (9)$$

where the function $\text{clip}(x, \min, \max)$ constrains x to the interval $[\min, \max]$. Here t , a scalar, is uniformly distributed as $t \sim \mathcal{U}(0, 1)$. z denotes pure Gaussian noise, follows a D -dimensional normal distribution, $z \sim \mathcal{N}(0, I)$, with $z \in \mathbb{R}^D$. $s \in \mathbb{R}$ is a scale hyperparameter. As outlined in Definition 1, given that $a_0^d(t) + a_1^d(t) = 1$, the determination of $a_1^d(t)$ defines $\alpha^d(t)$.

This approach is straightforward yet fails to consider the values between adjacent pixels in images, which are crucial for maintaining the structural integrity of the data. If the scale parameter s is large, it can result in significant differences between adjacent pixel values, potentially hindering training. To mitigate this, we propose second interpolant constructed as follows:

Example 2. *The low-pass filtered interpolant is described by:*

$$a_1^D(t) = \text{clip}(t + s \cdot f^{LP}(u, G), 0, 1), \quad (10)$$

where $u \in \mathbb{R}^D$ is sampled from a uniform distribution over the interval $[0, 1]$ for each dimension, i.e., $u \sim \mathcal{U}(0, 1)$. The low-pass filter f^{LP} employs convolution with a Gaussian kernel G , formulated as:

$$f^{LP}(u, G) = 2 \frac{(u * G) - \min(u * G)}{\max(u * G) - \min(u * G)} - 1 \quad (11)$$

Here, the $*$ denotes the convolution operation, and the result of $u * G$ is normalized to the interval $[-1, 1]$. $s \in \mathbb{R}$ is also the scale hyperparameter.

As depicted in Figure 3, the low-pass filtered interpolant shows less variance between adjacent pixels compared to the Gaussian-noised interpolant. The variance of the multidimensional coefficients can be adjusted by modifying the scale parameter s .

Using the above interpolants, the model g_{θ_0} is trained with the following loss as dictated by Equation 7.

$$\mathcal{L}(\theta_0) = \sum_{k=0}^K \mathbb{E}_{t, x_0, x_1} [|g_{\theta_0, k}(\alpha^D(t), x(\alpha^D(t)))|^2 - 2x_k \cdot g_{\theta_0, k}(\alpha^D(t), x(\alpha^D(t)))], \quad K = 1. \quad (12)$$

4.2 Path optimization by simulation dynamics and adversarial training

Path optimization is treated as depicted in Figure 2. For simplicity, a first-order Euler solver is selected as the differential equation solver of choice. Since the Euler solver requires a velocity field b , we design a parameterized velocity field b and optimize the path with adversarial training.

Designing a learnable path Following the methodology proposed by Albergo et al. [5], we model the velocity field b by the coefficient $\alpha^d(x_0, t)$ through a Fourier expansion in t . Our approach, however, deviates from Albergo et al. [5] in two significant aspects: firstly, we extend the dimension of the time-dependent coefficient to $d = D$, and secondly, we model the Fourier coefficients via a neural network $p_{\theta_1}(x_0)$, which depends on $x_0 \sim \rho_0(x_0)$. These modifications allow for the generation of multidimensional paths conditioned on the initial state x_0 , thereby facilitating the discovery of more adaptive pathways.

The parameterized multidimensional coefficients, $\alpha_{\theta_1}^D(x_0, t)$, is given by:

$$\alpha_{\theta_1}^D(x_0, t) = (a_{\theta_1,0}^D(x_0, t), a_{\theta_1,1}^D(x_0, t)), \quad (13)$$

where $a_{\theta_1,0}^D(x_0, t)$ and $a_{\theta_1,1}^D(x_0, t)$ are determined by the relations:

$$a_{\theta_1,0}^D(x_0, t) = \frac{\tilde{a}_0}{\tilde{a}_0 + \tilde{a}_1}, \quad (14)$$

$$a_{\theta_1,1}^D(x_0, t) = \frac{\tilde{a}_1}{\tilde{a}_0 + \tilde{a}_1}. \quad (15)$$

Here, \tilde{a}_0 and \tilde{a}_1 denote $\tilde{a}_{\theta_1,0}^D(x_0, t)$ and $\tilde{a}_{\theta_1,1}^D(x_0, t)$ respectively, and are defined as:

$$\tilde{a}_{\theta_1,0}^D(x_0, t) = 1 - t + \left(\sum_{m=1}^M p_{\theta_1,0,m}(x_0) \cdot \sin(\pi mt) \right)^2, \quad (16)$$

$$\tilde{a}_{\theta_1,1}^D(x_0, t) = t + \left(\sum_{m=1}^M p_{\theta_1,1,m}(x_0) \cdot \sin(\pi mt) \right)^2, \quad (17)$$

where M is the Fourier basis count. Then, the velocity field, $b_{\theta_0, \theta_1}(t, x, x_0)$, can be written as:

$$b_{\theta_0, \theta_1}(t, x, x_0) = \dot{a}_{\theta_1,0}^D(x_0, t) \cdot g_{\theta_0,0}(\alpha_{\theta_1}^D(x_0, t), x) + \dot{a}_{\theta_1,1}^D(x_0, t) \cdot g_{\theta_0,1}(\alpha_{\theta_1}^D(x_0, t), x). \quad (18)$$

Adversarial training with simulation dynamics We employ b_{θ_0, θ_1} along with a first-order Euler solver to render predictions dynamically through simulation dynamics. Subsequently, both the predictions and the ground truth image x_0 go into a discriminator for GAN-based adversarial training [6]. The following is the pseudo code for the described process:

Algorithm 1 Path optimization with a first-order Euler solver

```

1: repeat
2:   Sample  $x_0 \sim \mathcal{N}(0, I)$ ,  $x_1 \sim \rho_1(x_1)$ 
3:   Get  $p_{\theta_1}(x_0)$ 
4:   Initialize  $x \leftarrow x_0$ 
5:   for  $n = 0$  to  $N - 1$  do
6:      $t \leftarrow \frac{n}{N}$ 
7:     Calculate  $\alpha_{\theta_1}^D(x_0, t)$ ,  $\dot{\alpha}_{\theta_1}^D(x_0, t)$  using  $p_{\theta_1}(x_0)$ 
8:     Get  $g_{\theta_0}(\alpha_{\theta_1}^D(x_0, t), x)$ 
9:     Calculate  $b_{\theta_0, \theta_1}(t, x, x_0)$  using  $\alpha_{\theta_1}^D(x_0, t)$ ,  $\dot{\alpha}_{\theta_1}^D(x_0, t)$ , and  $g_{\theta_0}(\alpha_{\theta_1}^D(x_0, t), x)$ 
10:    Update  $x \leftarrow x + \frac{1}{N} b_{\theta_0, \theta_1}(t, x, x_0)$ 
11:  end for
12:  Get  $D_{\theta_2}(x)$ ,  $D_{\theta_2}(x_1)$ 
13:  Update parameters  $\theta_1, \theta_2$  using adversarial loss derived from  $D_{\theta_2}(x)$ ,  $D_{\theta_2}(x_1)$ 
14: until convergence

```

Here, N specifies the NFE of Euler solver, and D_{θ_2} represents the discriminator. By freezing parameter θ_0 and optimizing only θ_1 and θ_2 , optimization is focused solely on the path.

Table 1: FID-50k scores computed using an Euler solver, indicating better performance with smaller numbers. SI_{basic} applies the stochastic interpolant directly, while $SI_{modified}$, for a fair comparison, adopts the multidimensional interpolant’s conditioning approach as detailed in Section 5.1. The GNI (Gaussian-noised interpolant) and $LPFI$ (low-pass filtered interpolant) vary by scale parameters s , as explained in Examples 1 and 2.

NFE	10	20	30	40	50	100	150	200
Linear path								
SI_{basic}	17.20	7.20	5.73	5.37	5.23	4.82	4.55	4.38
$SI_{modified}$	19.14	7.27	5.61	5.27	5.13	4.81	4.56	4.40
$GNI_{s=0.005}$	11.73	7.40	6.36	5.75	5.35	4.10	3.77	3.66
$GNI_{s=0.02}$	16.84	6.30	4.75	4.77	5.10	8.41	9.52	10.13
$LPFI_{s=0.005}$	15.85	7.04	5.97	5.64	5.49	4.88	4.56	4.37
$LPFI_{s=0.1}$	14.18	8.92	7.34	6.36	5.61	3.79	3.71	3.76
Adaptive path								
$LPFI_{s=0.1}$	8.58	6.53	-	-	4.22	-	-	-

5 Experiments

To empirically validate the efficacy of multidimensional interpolants, we conduct experiments on the CIFAR-10 dataset, focusing on measuring the Fréchet Inception Distance (FID) scores. Initially, employing methodologies introduced in Section 4.1, we train g_{θ_0} across various scale parameters s , comparing its performance against baseline stochastic interpolants with linear paths, using a range of step numbers for a comprehensive analysis. Subsequently, we execute path optimization using a different number of function evaluations (NFE) with the Euler solver, as described in Section 4.2, and assess the results before and after path optimization.

5.1 Implementation details

For the configuration of g_{θ_0} , we use a UNet structure, as described by Dhariwal and Nichol [12]. Due to the expansion of the interpolation coefficient’s dimension to D , the conventional method of conditioning the interpolation coefficient $\alpha^1(t)$ for g_{θ_0} becomes inapplicable. Instead, we adopt a straightforward approach by concatenating the multidimensional coefficients $\alpha^D(t)$ with the interpolated value $x(\alpha^D(t))$ along the channel axis, forming an input dimension of $[B, 2C, H, W]$ for g_{θ_0} . The outputs of g_{θ_0} and p_{θ_1} , namely $g_{\theta_0,0}, g_{\theta_0,1}$, and $p_{\theta_1,0}, p_{\theta_1,1}$, are organized along the channel axis. Our training implementations reference the code provided by Tong et al. [8, 9]. Training occurs on a single GPU, either NVIDIA’s RTX 3080Ti or A6000, using a polynomial decaying learning rate scheduler with a peak learning rate of 2×10^{-4} . Specifically, g_{θ_0} trains with a batch size of 128 for 400,000 training steps, including 5,000 warm-up steps. The Adam optimizer is utilized throughout all training phases. FID scores are calculated using PyTorch-FID [13].

5.2 Results

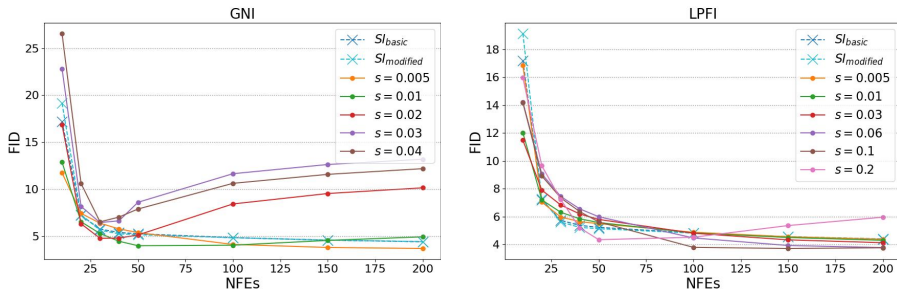


Figure 4: FID scores for a linear path against varying numbers of function evaluations (NFE) for different scale parameters s . As s increases, GNI on the left exhibits an increase in FID scores at higher NFE. In contrast, despite using relatively large values of s , LPFI on the right demonstrates a consistent decrease in FID scores as NFE increases.

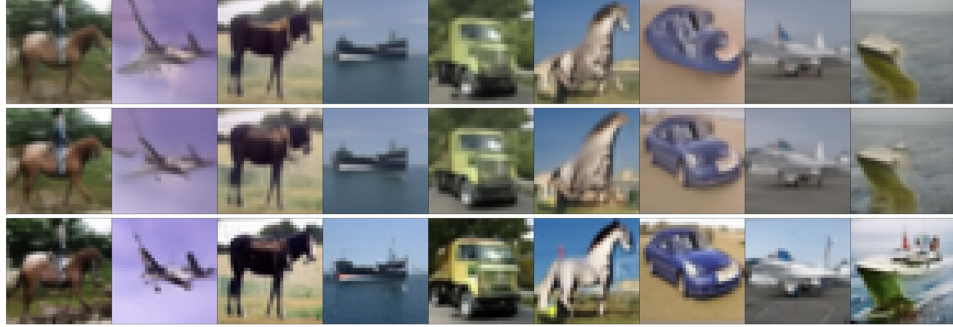


Figure 5: Comparison of results: stochastic interpolant applied to linear paths (first row), multidimensional interpolant applied to linear paths (second row), and adaptive paths (third row).

Table 1 presents the results of measuring FID scores for a linear path using both stochastic and multidimensional interpolants. Interestingly, some multidimensional interpolants exhibit higher performance compared to those utilizing a scalar interpolation coefficient in stochastic interpolants, even when using a linear path without path optimization. The use of multidimensional interpolants augments the model input, broadening the learning space. Nevertheless, the observed improvement in FID scores indicates that multidimensional interpolants do not overload the model but can instead positively influence the training of g_{θ_0} . However, not all multidimensional interpolants achieve higher FID scores than the baselines, as evidenced by Figure 4. GNI for $s > 0.01$ do not show a clear trade-off between NFE and FID; rather, an increase in NFE corresponds to higher FID scores. In contrast, LPFI, even with relatively large scale values compared to GNI, consistently show a reduction in FID scores as NFE increases. This suggests that the appropriate design of multidimensional interpolants can stably enhance model performance, even without path optimization.

For path optimization, g_{θ_0} trained with LPFI and a scale parameter of $s = 0.1$ is used. Table 1 presents the FID scores resulting from path optimization, consistently showing lower FID scores compared to a linear path. In Figure 5, we compare the baseline stochastic interpolant and the multidimensional interpolant using an Euler solver over 10 steps, starting from the same initial point x_0 . Qualitatively, following an adaptive path leads to the generation of the most interpretable images. Therefore, we can empirically state that this optimized multidimensional adaptive path achieves better performance compared to scalar-valued linear paths using the same solver and NFE.

6 Conclusion

In this study, we depart from the conventional use of single-dimensional interpolation coefficients in differential equation-based generative models by introducing a methodology that employs multidimensional interpolation coefficients. We also develop an algorithm that identifies adaptive multidimensional paths under fixed solver and NFE conditions. Our experimental results show that adaptive multidimensional interpolation coefficients surpass conventional methods relying on single-dimensional coefficients. We anticipate that our approach will pave the way for future research in this field.

References

- [1] Yaron Lipman, Ricky T. Q. Chen, Heli Ben-Hamu, Maximilian Nickel, and Matthew Le. Flow matching for generative modeling. In *The Eleventh International Conference on Learning Representations*, 2023. URL <https://openreview.net/forum?id=PqvMRDCJT9t>.
- [2] Xingchao Liu, Chengyue Gong, and qiang liu. Flow straight and fast: Learning to generate and transfer data with rectified flow. In *The Eleventh International Conference on Learning Representations*, 2023. URL <https://openreview.net/forum?id=XVjTT1nw5z>.
- [3] Yang Song, Jascha Sohl-Dickstein, Diederik P Kingma, Abhishek Kumar, Stefano Ermon, and Ben Poole. Score-based generative modeling through stochastic differential equations. In

- International Conference on Learning Representations*, 2021. URL <https://openreview.net/forum?id=PXTIG12RRHS>.
- [4] Michael S Albergo, Nicholas M Boffi, and Eric Vanden-Eijnden. Stochastic interpolants: A unifying framework for flows and diffusions. *arXiv preprint arXiv:2303.08797*, 2023.
 - [5] Michael Samuel Albergo, Nicholas Matthew Boffi, Michael Lindsey, and Eric Vanden-Eijnden. Multimarginal generative modeling with stochastic interpolants. In *The Twelfth International Conference on Learning Representations*, 2024. URL <https://openreview.net/forum?id=FHQAzW12wE>.
 - [6] Ian Goodfellow, Jean Pouget-Abadie, Mehdi Mirza, Bing Xu, David Warde-Farley, Sherjil Ozair, Aaron Courville, and Yoshua Bengio. Generative adversarial nets. In Z. Ghahramani, M. Welling, C. Cortes, N. Lawrence, and K.Q. Weinberger, editors, *Advances in Neural Information Processing Systems*, volume 27. Curran Associates, Inc., 2014. URL https://proceedings.neurips.cc/paper_files/paper/2014/file/5ca3e9b122f61f8f06494c97b1afccf3-Paper.pdf.
 - [7] Ricky T. Q. Chen, Yulia Rubanova, Jesse Bettencourt, and David K Duvenaud. Neural ordinary differential equations. In S. Bengio, H. Wallach, H. Larochelle, K. Grauman, N. Cesa-Bianchi, and R. Garnett, editors, *Advances in Neural Information Processing Systems*, volume 31. Curran Associates, Inc., 2018. URL https://proceedings.neurips.cc/paper_files/paper/2018/file/69386f6bb1dfed68692a24c8686939b9-Paper.pdf.
 - [8] Alexander Tong, Nikolay Malkin, Kilian FATRAS, Lazar Atanackovic, Yanlei Zhang, Guillaume Hugué, Guy Wolf, and Yoshua Bengio. Simulation-free schrödinger bridges via score and flow matching. In *ICML Workshop on New Frontiers in Learning, Control, and Dynamical Systems*, 2023. URL <https://openreview.net/forum?id=adj23mvB0>.
 - [9] Alexander Tong, Kilian FATRAS, Nikolay Malkin, Guillaume Hugué, Yanlei Zhang, Jarrid Rector-Brooks, Guy Wolf, and Yoshua Bengio. Improving and generalizing flow-based generative models with minibatch optimal transport. *Transactions on Machine Learning Research*, 2024. ISSN 2835-8856. URL <https://openreview.net/forum?id=CD9Snc73AW>. Expert Certification.
 - [10] Mark Goldstein, Michael Samuel Albergo, Nicholas Matthew Boffi, Rajesh Ranganath, and Eric Vanden-Eijnden. Stochastic interpolants with data-dependent couplings, 2024. URL <https://openreview.net/forum?id=fK9RkJ4fgo>.
 - [11] Neta Shaul, Ricky T. Q. Chen, Maximilian Nickel, Matthew Le, and Yaron Lipman. On kinetic optimal probability paths for generative models. In Andreas Krause, Emma Brunskill, Kyunghyun Cho, Barbara Engelhardt, Sivan Sabato, and Jonathan Scarlett, editors, *Proceedings of the 40th International Conference on Machine Learning*, volume 202 of *Proceedings of Machine Learning Research*, pages 30883–30907. PMLR, 23–29 Jul 2023. URL <https://proceedings.mlr.press/v202/shaul23a.html>.
 - [12] Prafulla Dhariwal and Alexander Nichol. Diffusion models beat gans on image synthesis. In M. Ranzato, A. Beygelzimer, Y. Dauphin, P.S. Liang, and J. Wortman Vaughan, editors, *Advances in Neural Information Processing Systems*, volume 34, pages 8780–8794. Curran Associates, Inc., 2021. URL https://proceedings.neurips.cc/paper_files/paper/2021/file/49ad23d1ec9fa4bd8d77d02681df5cfa-Paper.pdf.
 - [13] PyTorch implementation of FID. <https://github.com/mseitzer/pytorch-fid>.